Liquid crystal spatial light modulator with very large phase modulation operating in high harmonic orders

Venancio Calero,[1] Pascuala García-Martínez,[2] Jorge Albero,[3] María M. Sánchez-López,[4] and Ignacio Moreno[1,*]

[1]*Departamento de Ciencia de Materiales, Óptica y Tecnología Electrónica, Universidad Miguel Hernández, 03202 Elche, Spain*

[2]*Departamento de Óptica, Universitat de València, 46100 Burjassot, Spain*

[3]*Département Micro Nano Sciences et Systèmes, Institute FEMTO-ST (UMR CNRS 6174), Université de Franche-Comté, 16 Route de Gray, 25030 Besançon cedex, France*

[4]*Instituto de Bioingeniería, Universidad Miguel Hernández, 03202 Elche, Spain*

**Corresponding author: i.moreno@umh.es*

Received July 31, 2013; revised October 9, 2013; accepted October 9, 2013;
posted October 9, 2013 (Doc. ID 195012); published November 8, 2013

Unusually large phase modulation in a commercial liquid crystal spatial light modulator (LCSLM) is reported. Such a situation is obtained by illuminating with visible light a device designed to operate in the infrared range. The phase modulation range reaches 6π radians in the red region of the visible spectrum and 10π radians in the blue region. Excellent diffraction efficiency in high harmonic orders is demonstrated despite a concomitant and non-negligible Fabry–Perot interference effect. This type of SLM opens the possibility to implement diffractive elements with reduced chromatic dispersion or chromatic control. © 2013 Optical Society of America

OCIS codes: (070.6120) Spatial light modulators; (050.1970) Diffractive optics; (060.5060) Phase modulation.
http://dx.doi.org/10.1364/OL.38.004663

Diffractive optical elements (DOEs) play an important role in many optical technologies [1]. Liquid crystal (LC) spatial light modulators (SLMs) are useful devices for implementing a variety of programmable DOE, mainly when they produce pure-phase modulation characteristics [2]. Usually, a phase-modulation range reaching 2π radians is desired, which has been achieved easily in earlier devices [3,4]. The resolution and response time of LC modulators depends on several factors, such as the cell gap, the LC visco-elastic coefficient, and the gray-to-gray voltage [5]. The goal of reaching higher resolution and faster optical responses led to a reduction of the LC layer thickness in modern devices. This layer reduction is not a problem for amplitude modulation display applications, but it reduces significantly the overall phase modulation range. In many LC transmission devices, the available phase dynamic range is actually shorter than 2π radians in standard configurations. Strategies have been demonstrated either to optimally encode a phase-DOE onto a limited phase modulation device [6], or to enlarge the phase modulation range by using unconventional polarization configurations, although this improvement comes at the expense of a reduction in the average intensity transmission [7,8].

Modern LC on Silicon (LCoS) modulators work in reflection, thus providing higher values of the phase modulation range. Therefore, phase-only LC devices with phase modulation range larger than 2π are nowadays commercially available. We recently examined the diffraction properties of two-dimensional DOEs displayed in a parallel-aligned LCoS display with a dynamic phase range reaching 4π radians for $\lambda = 454$ nm. This doubled phase depth, compared to standard 2π phase modulation, allows DOEs to be operated in the second harmonic diffraction order [9]. This type of operation shows important advantages to overcome the limits of spatial resolution introduced by the diffraction efficiency reduction caused by the fringing field effect. This effect can be relevant especially in devices with small pixels or with thick LC layers [10].

However, reaching even higher values of phase modulation is very interesting in order to reproduce DOEs with specific chromatic control. For instance, color separation gratings were proposed in [11]. Other examples are multi-order [12] and harmonic [13] diffractive lenses, which are higher order generalizations of the usual modulo 2π blazed diffractive lens. These types of elements have not been encoded with SLMs, because they require high phase modulation values. As an alternative to the common 2π phase modulation, in this Letter we are able to implement phase modulation DOEs with phase dynamic range between 6π and 10π for wavelengths in the visible range.

We have been using parallel-aligned nematic LC devices from Hamamatsu LCoS-SLM (X10468 series), with 792×600 pixels of size 20×20 μm^2 and refreshing rates of 60 Hz (with rise times of 30 ms). The device employed in [9] was designed to be operated in the visible (VIS) range from 400 to 700 nm. However, the same device series proposes another model (X10468-08) with the same characteristics but designed to work in the infrared (IR) range, from 1000 to 1500 nm. This device, therefore, is expected to introduce higher phase values in order to compensate the phase reduction due to the use of longer wavelengths. As an unusual novelty, we thus examined the phase modulation properties of such device operating in the VIS range.

The input beam was selected linearly polarized along the LC director axis, in order to obtain a phase-only modulation output. We operated the device for three wavelengths in the VIS range, $\lambda = 633$ nm of a He–Ne laser, and $\lambda = 514$ nm and $\lambda = 454$ nm of a tunable Ar ion laser. Figure 1 shows the reflected intensity measured with a photodetector for these three wavelengths, when the addressed gray level is changed from 0 to 255. The curves are normalized with respect to the intensity of the input beam. An oscillation is observed, which is characteristic of a Fabry–Perot interference of multiple reflections on the device [14]. These oscillations are

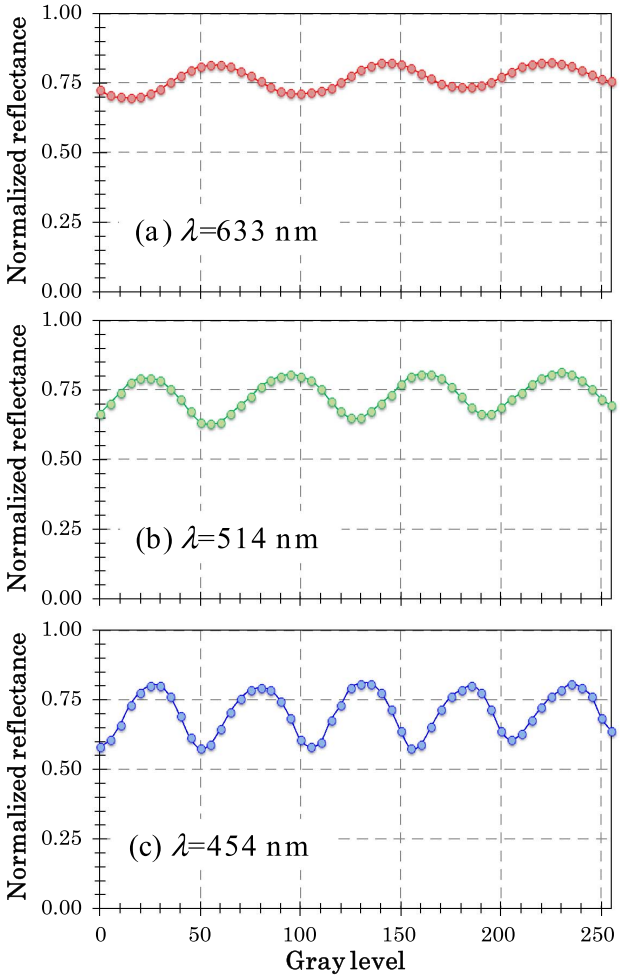

Fig. 1. Normalized reflectance as a function of the addressed gray level for wavelengths of (a) 633 nm, (b) 514 nm, and (c) 454 nm. Input polarization is selected parallel to the LC director.

faster as the wavelength decreases. Reflectance maxima are obtained whenever the phase shift gained in the round trip propagation inside the LC layer is an even multiple integer of π radians. On the contrary, reflectance minima occur when the phase shift in the LC layer is an odd multiple of π radians.

Thus, the results in Fig. 1 show approximately three, four, and five complete oscillations for wavelengths of 633, 514, and 454 nm, respectively. This indicates that the corresponding phase modulation approximates 6π, 8π, and 10π, respectively. The fact of providing larger phase shift values for shorter wavelengths is due to the λ^{-1} dependence of the phase function, as well as to the LC refractive indices dispersion [15]. The phase ranges achieved here are unusually large in modern SLM technology, since LC devices for display applications in the visible range have followed the tendency to reduce the thickness of the LC layer to improve switching speed. The fact that this device was designed to work with IR light, indicates that the LC layer must be thicker than that of devices designed for VIS light. However, a device with such large phase variation is very interesting for VIS light since it can be used to display multi-order harmonic diffractive elements. Namely, this high phase range makes possible to operate this SLM up to the third, fourth, and fifth diffraction orders for 633, 514, and 454 nm, respectively (note that in [9] the maximum operation was only in the second order).

In order to show these higher harmonic diffractive orders, we have experimentally generated blazed gratings. As demonstrated in [9], if a blazed grating is made with phase modulation range from zero to a maximum phase value $\Phi_{\max} = M2\pi$, the light intensity at the Fourier diffraction plane is progressively shifted to higher diffraction orders. Here M is a real positive number that accounts for the maximum phase shift. $M = 0$ is equivalent to the absence of the grating, and all the light remains at the zero order. For $M \neq 0$, other diffraction orders appear with a relative intensity given by $I_n = \mathrm{sinc}^2(n - M)$, where n denotes the diffraction order, and the sinc function is defined as $\mathrm{sinc}(x) = \sin(\pi x)/(\pi x)$.

For $M = 0.5$ ($\Phi_{\max} = \pi$), the most intense orders are $n = 0$ and $n = 1$, with $I_0 = I_1 = 40.5\%$. For $M = 1$ ($\Phi_{\max} = 2\pi$), the usual blazed grating is reproduced, and all the intensity is now shifted to the positive first order, with maximum efficiency ($I_1 = 100\%$), while the other diffraction orders vanish. Larger integer values of M lead once again to maximum 100% efficiency, but at higher diffraction orders given by $n = M$. For semi-integer values, $M = (m + 1/2)$, the maximum phase shift $\Phi_{\max}$ reaches an odd integer value of π radians, $\Phi_{\max} = (2m + 1)\pi$, and the light intensity is mostly distributed among two consecutive diffraction orders $n = m$ and $n = m + 1$, with relative intensities $I_m = I_{m+1} = 40.5\%$.

Figure 2 shows the obtained experimental results for the wavelength of 514 nm. It can be seen how the light beam, initially concentrated in the zero diffraction order in the absence of blazed grating, is progressively shifted to $n = +1$, $+2$, $+3$, and finally $+4$ diffraction orders. Whenever the phase modulation reaches an odd integer number of π radians, light is mainly split into two consecutive diffraction orders, while it is concentrated on a single diffraction order when the phase modulation range reaches an even integer number of π radians. Similar results have been observed for 633 nm and for 454 nm. In those cases, the third and fifth diffraction order were attained, respectively. Note that some secondary effects may affect the diffraction efficiency considerations described above. For instance, the Fabry–Perot effect in Fig. 1 creates an amplitude modulation coupled to the phase modulation. In addition, quantization levels affect differently as the phase modulation range increases. Nevertheless, the results in Fig. 2 show the dominant behavior of the large phase modulation. Interesting applications of nonmechanical beam steering can be exploited thanks to this capability of addressing a large number of steering angles with high light efficiency. Note that the modulation diffraction efficiency, as defined in [6], reaches values close to the ideal 100%. Nevertheless, other sources of diffraction efficiency loss, like absorption, or multiple diffraction caused by the pixelated structure of the device, reduce the overall efficiency to a maximum factor of approximately 70%.

An additional experiment was performed to show the potential of such unusual large phase modulation when operating with polychromatic illumination. Figure 3 displays two composed images of the diffraction plane,

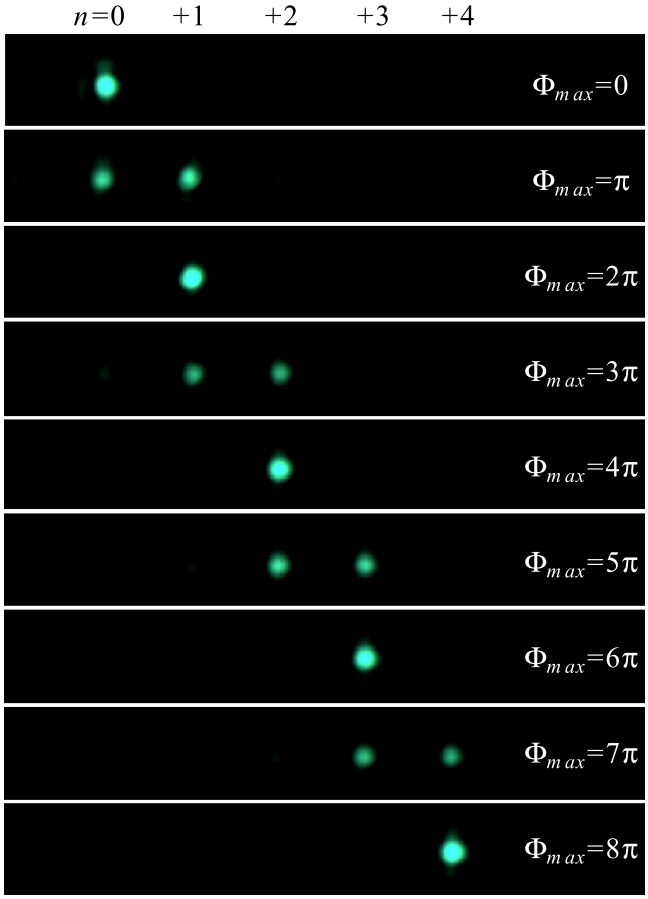

Fig. 2. Diffraction pattern as a function of the maximum phase shift Φ_{max} of a blazed grating when it is growing from zero to 8π radians. Light intensity is progressively transferred from zero to fourth diffraction order.

obtained by superimposing the three patterns captured when illuminating the blazed grating with wavelengths 633, 514, and 454 nm, respectively. An achromatic lens was used to focus the diffraction plane onto a color CCD camera. In Fig. 3(a), the phase modulation range was adjusted to be 2π for each wavelength, i.e., the LCSLM is operated in the usual first diffraction order. Each wavelength produces mainly a first diffraction order, whose location follows the typical chromatic dispersion, where larger wavelengths are diffracted onto larger diffraction angles. Some amount of light appears on the zero diffraction order due to the intensity modulation shown in Fig. 1. Here the images are saturated and this zero order becomes more visible.

On the contrary, Fig. 3(b) shows the result when the LCSLM works with the maximum available phase dynamic range (the blazed grating is addressed with the maximum available gray level range from 0 to 255). Now the phase modulation ranges are 6π radians for $\lambda = 633$ nm, 8π for $\lambda = 514$ nm, and 10π for $\lambda = 454$ nm. Therefore, the blazed grating acts in the third, fourth, and fifth diffraction order, respectively. Since the larger wavelength operates in the lowest diffraction order, and vice versa, chromatic dispersion is notably reduced, as shown in Fig. 3(b). This is shown in Fig. 3(b). For the sake of comparison, the period of the blazed grating is four times larger than in Fig. 3(a), so the main diffraction

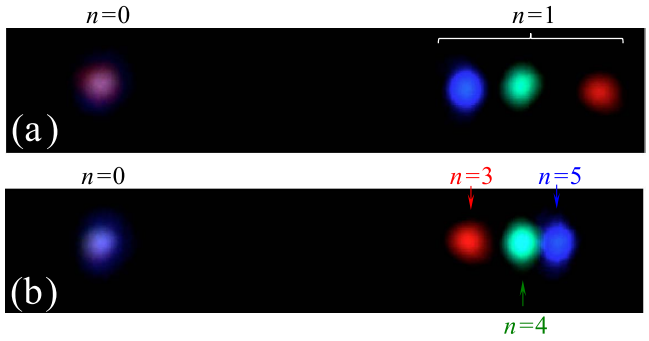

Fig. 3. Superposition of the diffraction patterns for wavelengths of 633, 514, and 454 nm for (a) blazed grating operating in the first diffraction order and (b) blazed grating operating in higher diffraction orders. For the sake of comparison, the grating in (a) has a period four times shorter compared to (b) in order to achieve the same diffraction angle for 514 nm.

order is located at the same angular position for the central wavelength of 514 nm. As it can be observed, the chromatic dispersion relation is inverted (the red light is diffracted with a smaller angle, and the blue light with a larger angle), and the global chromatic dispersion is reduced.

In order to numerically evaluate these two configurations, let us consider the diffraction grating law, $\sin\theta = n\lambda/p$, where p is the period of the grating and θ the diffraction angle. We consider as the reference value $s = \sin\theta$ for 514 nm (s_{514}), which coincides in the two cases with a period p for order $n = 1$ and with a period $4p$ for order $n = 4$. Table 1 gives the relative values s_{633}/s_{514} and s_{454}/s_{514} for the other two wavelengths, in the two cases of Fig. 3, i.e., for $n = 1$ with a period p, and for $n = 3$ (633 nm) and $n = 5$ (454 nm) for a period $4p$. The relative difference $\Delta s = (s_{633} - s_{454})/s_{514}$ is also given in Table 1, which serves as a measurement of the dispersion of the grating. The positive value of Δs in the configuration of Fig. 3(a) indicates the normal chromatic dispersion tendency observed in the figure. On the contrary, the negative value of Δs in the configuration of Fig. 3(b) confirms the experimentally observed inverted chromatic dispersion relation. In addition, the absolute value is reduced approximately to one half, ratifying the dispersion reduction observed in the experiment.

In conclusion, we have shown that the parallel-aligned Hamamatsu LCoS-SLM model X10468-08, initially designed to operate in the IR spectral range, can also be very useful to operate in the VIS range, because of its very large phase modulation. High dynamic phase range up to 6π radians for $\lambda = 633$ nm, to 8π for $\lambda = 514$ nm, and to 10π for $\lambda = 454$ nm has been shown, thus allowing

Table 1. Relative Ratio s/s_{514}, Being $s = \sin\theta$ and θ the Diffraction Angle, for the Two Gratings in Fig. 3 and for the Wavelengths of 633, 514, and 454 nm, Respectively

	Fig. 3(a)	Fig. 3(b)
	Period p $n = 1$	Period $4p$ $n = 3$ (633 nm), $n = 4$ (514 nm), $n = 5$ (454 nm)
$\lambda = 454$ nm	0.833	1.104
$\lambda = 514$ nm	1	1
$\lambda = 633$ nm	1.231	0.924
Δs	+0.348	−0.180

operation in the third, fourth, and fifth diffraction orders, respectively. These findings open the possibility to encode diffractive elements with specific chromatic control into LCSLMs, as the simple example presented in Fig. 3, which demonstrates a reduced chromatic dispersion for the main diffracted order. Other multi-order harmonic diffractive elements [11–13] could therefore be implemented in such type of SLMs.

We acknowledge financial support from Spanish Ministerio de Economía y Competitividad and FEDER funds through project FIS2012-39158-C02-02.

References

1. J. Goodman, *Introduction to Fourier Optics*, 3rd ed. (Roberts & Company, 2004).
2. P. Yeh and C. Gu, *Optics of Liquid Crystals Displays*, 2nd ed. (Wiley, 2010).
3. U. Efron, S.-T. Wu, and T. D. Bates, J. Opt. Soc. Am. B **3**, 247 (1986).
4. N. Konforti, E. Marom, and S.-T. Wu, Opt. Lett. **13**, 251 (1988).
5. S.-T. Wu, Appl. Opt. **28**, 48 (1989).
6. I. Moreno, C. Iemmi, A. Márquez, J. Campos, and M. J. Yzuel, Appl. Opt. **43**, 6278 (2004).
7. J. A. Davis, J. Nicolas, and A. Marquez, Appl. Opt. **41**, 4579 (2002).
8. J. L. Martínez, I. Moreno, J. A. Davis, T. J. Hernández, and K. P. McAuley, Appl. Opt. **49**, 5929 (2010).
9. J. Albero, P. García-Martínez, J. L. Martínez, and I. Moreno, Opt. Lasers Eng. **51**, 111 (2013).
10. K.-H. Fan-Chiang, S.-T. Wu, and S.-H. Chen, J. Disp. Technol. **1**, 304 (2005).
11. H. Dammann, Appl. Opt. **17**, 2273 (1978).
12. D. Faklis and G. M. Morris, Appl. Opt. **34**, 2462 (1995).
13. D. W. Sweeney and G. E. Sommargren, Appl. Opt. **34**, 2469 (1995).
14. J. A. Davis, P. Tsai, D. M. Cottrell, T. Sonehara, and J. Amako, Opt. Eng. **38**, 1051 (1999).
15. S.-T. Wu, Phys. Rev. A **33**, 1270 (1986).